International Journal of Mechanical, Industrial and Aerospace Sciences
ISSN: 2517-9950
Vol:8, No:5, 2014

Computational Analysis of the Scaling Effects on the Performance of an Axial Compressor

Junting Xiang, Jörg Uwe Schlüter, Fei Duan

***Abstract*—**The miniaturization of gas turbines promises many advantages. Miniature gas turbines can be used for local power generation or the propulsion of small aircraft, such as UAV and MAV. However, experience shows that the miniaturization of conventional gas turbines, which are optimized at their current large size, leads to a substantial loss of efficiency and performance at smaller scales. This may be due to a number of factors, such as the Reynolds-number effect, the increased heat transfer, and manufacturing tolerances. In the present work, we focus on computational investigations of the Reynolds number effect and the wall heat transfer on the performance of axial compressor during its size change. The NASA stage 35 compressor is selected as the configuration in this study and computational fluid dynamics (CFD) is used to carry out the miniaturization process and simulations. We perform parameter studies on the effect of Reynolds number and wall thermal conditions. Our results indicate a decrease of efficiency, if the compressor is miniaturized based on its original geometry due to the increase of viscous effects. The increased heat transfer through wall has only a small effect and will actually benefit compressor performance based on our study.

***Keywords*—**Axial compressor, CFD, heat transfer, miniature gas turbines, Reynolds number.

NOMENCLATURE

a	= Reynolds independent loss fraction
Dh	= Hydraulic diameter
n	= Reynolds ratio exponent
P	= Stagnation pressure (Pa)
P_r	= Pressure ratio
γ	= Ratio of specific heat (1.4)
Re	= Reynolds number
R_{ss}	= Rotor suction side
SF	= Scaling factor
S_{ps}	= Stator pressure side
T	= Temperature (K)
T_r	= Temperature ratio
$_{ad}$	= Adiabatic efficiency

Subscripts

1	= rotor inlet
3	= stator outlet
ref	= reference value

Junting Xiang and Dr. Jörg Uwe Schlüter are with the Division of Aerospace Engineering, Nanyang Technological University, Singapore (e-mail: junting.xiang1988@gmail.com, schluter@ntu.edu.sg).

Dr. Fei Duan is with the Division of Thermal and Fluids Engineering, Nanyang Technological University, Singapore (e-mail: feiduan@ntu.edu.sg).

I. INTRODUCTION

GAS turbine engine study has always been of undeniable significance and interest among industry and academy, ever since the proposal of its concept. It is widely used to power aircraft, ships, trains or generators, etc., because of its advantages such as high power-to-weight ratio, comparatively small sizes, availability for various fuels, and such other advantages. Several types of gas turbines have been developed and realized in practice in order to fulfill different application requirements. Advantages and disadvantages exist simultaneously for every engine, thus a compromised selection should be reached. Fig. 1 shows the cutaway view of an axial gas turbine engine.

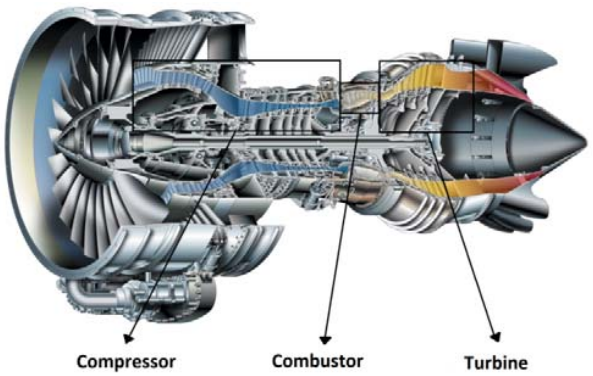

Fig. 1 An axial gas turbine

With the increasing demand for small and high performance engines, especially for unmanned aerial vehicles (UAV), the understanding of the scaling effects on the performance of engine components needs to be studied more closely. The aerodynamic behavior and general performance will change when engine size changes, thus a redesign and optimization of each component should be considered, based on the study of their working conditions. In this study, the performance of axial compressor in a gas turbine engine is investigated. It is an essential part in the engine operation cycle, as the compressor provides higher operating pressure for the combustor and thus a higher energy density. However, simply scaling down the original compressor from a conventionally sized engine will not necessarily provide sufficient pressure increase to meet the requirement for the pressure ratio per stage, in particular, as small gas turbines are usually geometrically simpler and need to work with fewer compressor stages.

Previous studies have presented investigations on some of the factors that affect the compressor performance. Wang and Hu (2004) have studied the stability and performance of axial fans and compressors with regards to the effects of Reynolds number. They have experimentally validated the performance variation and stability of compressors, indicating that both of these criteria deteriorate with decreasing Reynolds number [1]. Choi and Baek (2008) have considered the loss characteristics in an axial compressor due to the effects of low Reynolds number. Their study indicates that hub boundary layer and suction surface separation, caused by the low Reynolds number, reduce the static pressure rise and compressor performance [2]. Back and Hobson (2010) have focused on the relation between surface roughness and Reynolds number in compressor cascade performance. They found that the rough surface area, roughness location and Reynolds number interactively contribute to the loss coefficient [3]. Besides that, Casey and Robinson (2011) have made endeavor to derive a correction equation, which relates changes in compressor efficiency with Reynolds number to changes in surface roughness [4]. Recently, Zheng and Lin (2013) have investigated the Reynolds number effect on a high pressure ratio turbocharger compressor. Their results show that compressor efficiency and pressure ratio decrease by 6.9% and 7.9%, respectively, when Reynolds number drops from 9.86×10^5 to 2.96×10^5, based on their experimental and numerical results [5].

The heat transfer effect is another concern during compressor operation. In the miniaturization of the gas turbine, the surface to volume ratio increases and hence, more heat losses are to be expected. The majority of available literature focuses on the effect of heat transfer on the performance of the whole gas turbine engine cycle as the heat losses in the combustor are of particular importance [6]-[8]. Specific research regarding wall heat flux effect and internal flow heat exchange for compressor is rare. Although Ma and Xi (2010) have studied the heat transfer and Reynolds number effect on scaling of a centrifugal compressor impeller [9], more thorough study on wall heat flux effects is still required for engineering guidance.

Although extensive endeavors have been made to understand compressor performance, the knowledge about the factors impacting axial compressor performance during its scaling process is still in demand. Computational methods have taken great steps in the prediction of gas turbine performance [10]. In this work, parameter studies on the influence of Reynolds number and wall thermal conditions are studied numerically, to investigate the effects of these factors during the scaling process of an axial compressor.

II. Numerical Approach

A. Geometry & Mesh

The NASA stage 35 compressor is chosen as the test case model, as it is a well-documented experiment [11], [12]. The compressor design parameters and the radial cross sectional view of compressor flow passage are shown in Table I & Fig. 2 respectively. In total, 36 rotor blades and 46 stator blades compose the full circular of the compressors. Fig. 3 gives the geometric view of full circular compressor used in this study. However, due to concerns about computational time and resources, only one blade passage is meshed and used for subsequent computational approach, to represent the full circular during this numerical study. Thus rotor fluid passage with 10 degrees and stator fluid passage with 7.83 degrees are used, with periodic boundary condition applied in azimuthal direction.

TABLE I
Design Parameters for Stage 35 Compressors

Total Pressure Ratio	1.82
Total Temperature Ratio	1.225
Adiabatic Efficiency	0.828
Polytropic Efficiency	0.842
Flow Coefficient	0.451
Airflow	20.188
RPM at 100% Design Speed	17188.7
Tip Speed	454.456
Hub-Tip Radius Ratio	0.7
Rotor Aspect Ratio	1.19
Stator Aspect Ratio	1.26
Number of Rotor Blades	36
Number of Stator Blades	46

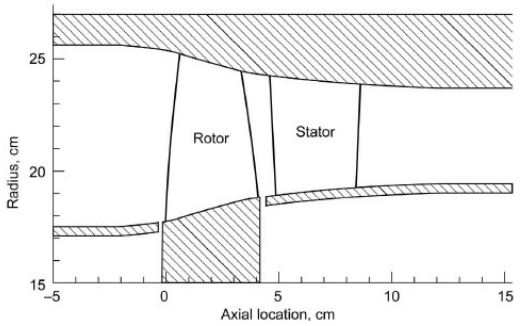

Fig. 2 Cross sectional view of compressor flow passage [13]

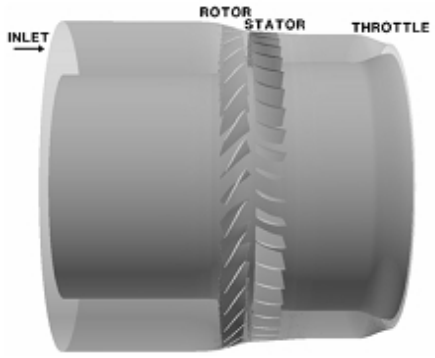

Fig. 3 Geometric view of full circular stage 35 compressor

A multi-block structured mesh is generated for the computational domain using the software Gambit 2.4. The tip clearance gap is not considered in this study, though certain research about it is available [14], [15]. The grid is formed separately for the rotor and stator fluid domain. Mesh refinements are conducted near blade leading and trailing edge

regions. Near wall treatment is also employed and a y+ value is adapted to 1. Our grid independence study suggests that 1.34 million mesh cells are sufficient in producing sufficiently accurate results. The computational grids for only rotor & stator domain are presented in Fig. 4.

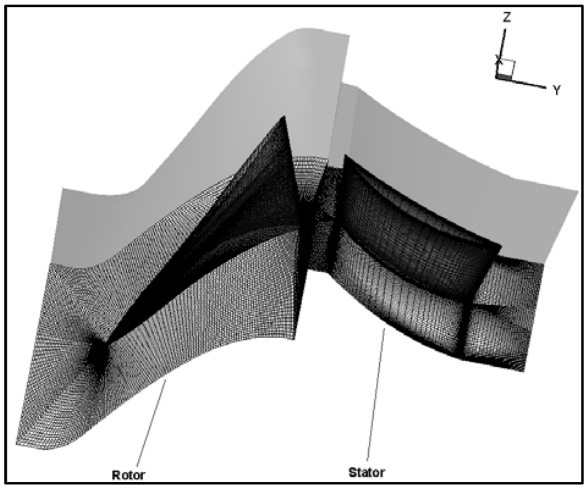

Fig. 4 Computational grid for rotor & stator domain

B. Boundary Condition & Numerical Scheme

Simulations are conducted in the commercial code ANSYS Fluent 13.0. Mass flow inlet boundary and pressure out outlet boundary conditions are applied. A specific mass flow rate of 172.6kg/m2×s, corresponding to a mass flow rate of 0.56kg/s is used, by a conversion of 1/36 of the designed total mass flow for this case. The initial gauge pressure values are defined respectively for inlet & outlet boundaries, based on experimental data. Periodic boundary conditions are implemented to both rotor & stator domain in the azimuthal direction and it represents the full circular by allowing fluid variables across the boundary continuously. All wall boundaries are defined as adiabatic for the initial case setup, though change in wall heat flux is applied in subsequent investigation in section Ⅳ. 100% design speed is applied to rotor domain while stator domain remains stationary. The mixing plane method is chosen to address the rotor-stator interaction, where flow data is circumferentially averaged. The Spalart-Allmaras turbulence model is selected from a preliminary validation study and engineering experience.

A steady state density based algorithm is used, which solves the continuity equation and momentum, energy, species transport as a coupled set of equations using an ideal gas. An implicit formulation is used for numerical solutions and 1st order upwind scheme is utilized to discretize both flow and turbulent viscosity. A small under relaxation factor value is used at the start of simulation to aid convergence. Each computation takes approximately 12 hours to reach the final convergence on 16 processors.

C. Numerical and Experimental Results

As a benchmark case for validation, we have generated the NASA stage 35 compressor mesh based on the original design parameters, resulting in an operating Reynolds number of 5.34×10^5.

The pressure distributions along compressor flow passage are presented in Fig. 5. A gradual increase of pressure value along flow passage is observed and peak pressure region is located near rotor shroud. A high pressure gradient can also be identified in the rotor fluid domain, when intake air is quickly compressed by the rotating rotor blade.

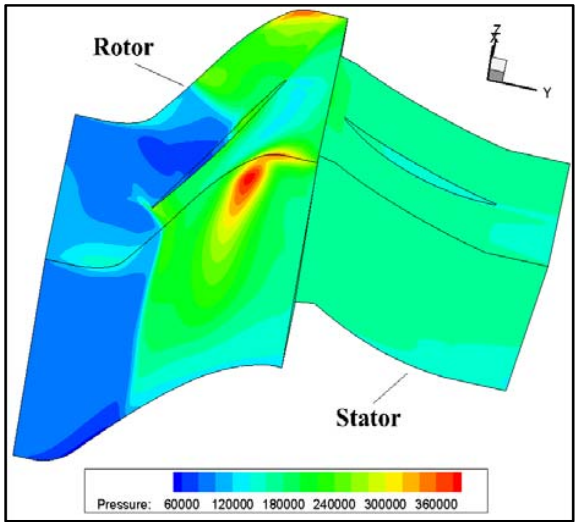

Fig. 5 Pressure distributions along flow passage for benchmark case at 100% design speed

The temperature distribution along flow passage is also shown in Fig. 6. The highest temperature region is located at rotor casing area, where friction between air and casing is tremendous. Flow separation might have occurred in rotor blade pressure side and it has leaded to the low temperature region identified. Fig. 7 shows the temperature increase from rotor hub towards casing in more details. The increased tangential speed has contributed to this variation.

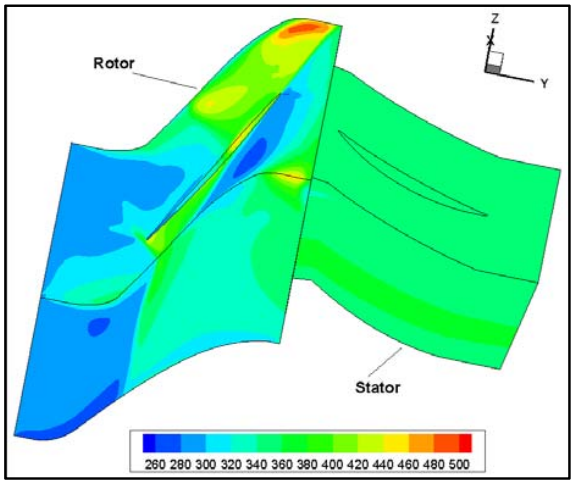

Fig. 6 Temperature distribution along flow passage for benchmark case at 100% design speed

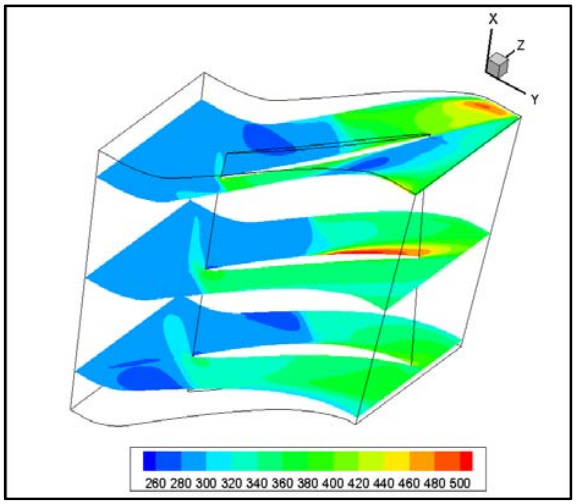

Fig. 7 Cross sectional view of rotor temperature distribution for benchmark case at 100% design speed

We have changed the mass flow rate at the compressor inlet and plotted the efficiency given as:

$$\eta_{ad} = \frac{(P_3/P_1)^{(\gamma-1)/\gamma}-1}{(T_3/T_1)-1} \quad (1)$$

with P_1 and T_1 the pressure and temperature at the inlet of the compressor, P_3 and T_3 the pressure and temperature at the outlet of the compressor, and γ the ratio of specific heat. This allows comparing our numerical results with experimental data [11].

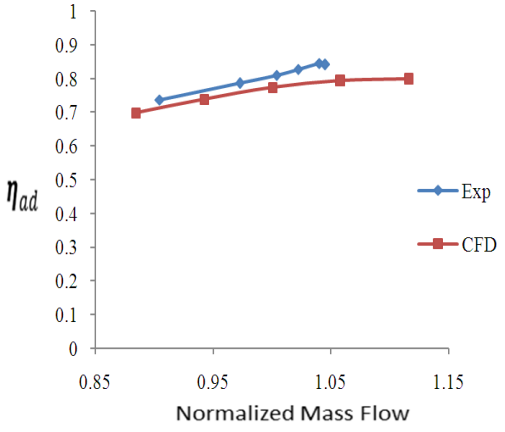

Fig. 8 Adiabatic efficiency variation with mass flow for benchmark case at 100% design speed

In Fig. 8, we compare the adiabatic efficiency of the experiment with our numerical results. As shown, the numerical results match the experimental results well, although it underestimates experiment value by about 4.5%. For both cases, the mass flow rate is normalized by the design airflow value, as previously given in Table I. Based on this comparison; we have shown that our simulations are sufficiently accurate for the subsequent study.

III. Reynolds Number Effect

We have applied scaling factors (SF) 1.6, 1.3, 0.7, and 0.4 on the geometry of the original complete test model, resulting in Reynolds numbers ranging from 8.54×10^5 to 2.14×10^5 at designed mass flow. The specific mass flow rate varies from 142.6kg/m^2×s to 202kg/m^2×s is then applied only on SF=1.6 and SF=0.4 cases for further comparison with benchmark case, in order to better understand compressor performance during its miniaturization process. We have also adjusted the rotor operation speed according to SF used to keep tip speed constant. Other boundary conditions remain unchanged as they are specified in the benchmark case. At the designed mass flow rate, the Reynolds Number only changes with the change of its hydraulic diameter. Table II presents specifications for different SF cases.

TABLE II
Specifications for Different SF Cases

Scaling Factor	Dh (m)	Specific mass flow(kg/m^2×s)	Reynolds Number
1.6	8.86×10^{-2}	172.6	8.54×10^5
1.3	7.20×10^{-2}	172.6	6.94×10^5
1	5.54×10^{-2}	172.6	5.34×10^5
0.7	3.87×10^{-2}	172.6	3.74×10^5
0.4	2.21×10^{-2}	172.6	2.14×10^5

A well-known empirical formula for efficiency correction, (2), is used for comparison of our computational results for Reynolds number effect study [16],

$$\frac{1-\eta_{ad}}{1-\eta_{ref}} = a + (1-a)[\frac{Re_{ref}}{Re}]^n \quad (2)$$

where "n" is empirically assumed to be 0.2 and "a" to be 0 for axial compressors. However, based on our study, a Reynolds ratio exponent "n" of 0.1 is able to better capture efficiency variation with Reynolds number. Fig. 9 shows the comparison of these two methods as well as our numerical results suggested correction.

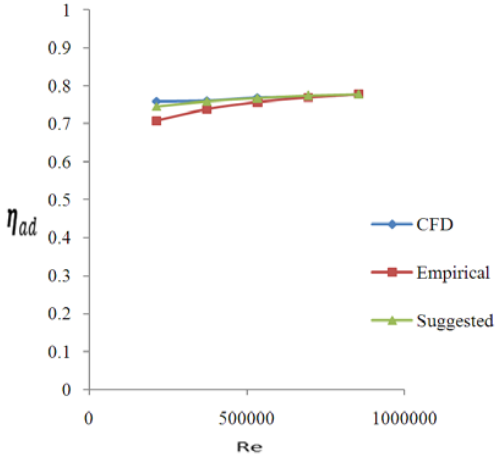

Fig. 9 Efficiency variations with Reynolds number at designed mass flow rate

As illustrated in Fig. 9, the adiabatic efficiency increases with the increase of Reynolds number within the scope of our study. This is shown by both the empirical formula and our study. Fig. 10 shows the change of efficiency with the variation of mass flow for three different SF cases. The mass flow is normalized with a designed value as shown in Table II. A maximum decrease of 1.3% of efficiency is observed when SF changes from 1.6 to 0.4. For all three cases, the highest efficiency point appears at 111.2% of designed mass flow.

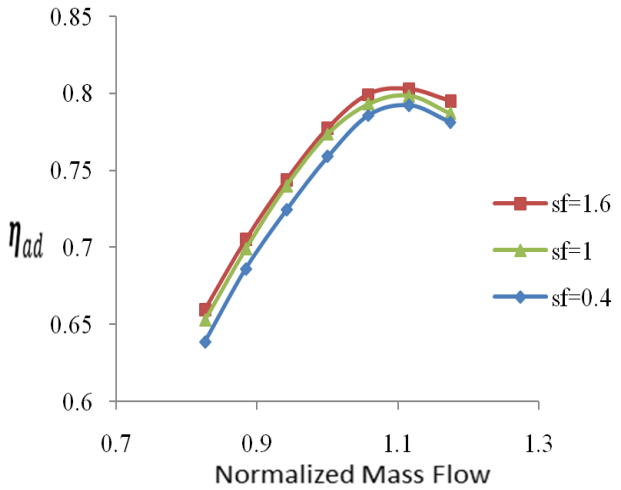

Fig. 10 Efficiency variations with mass flow for three SF cases

The pressure ratio changes with mass flow are also given in Fig. 11 for three SF cases. A general decrease of pressure is observed during the miniaturization process, with a largest pressure ratio drop of 1.42% when SF changes from 1.6 to 0.4. Highest pressure ratio point appears at designed mass flow for all three cases.

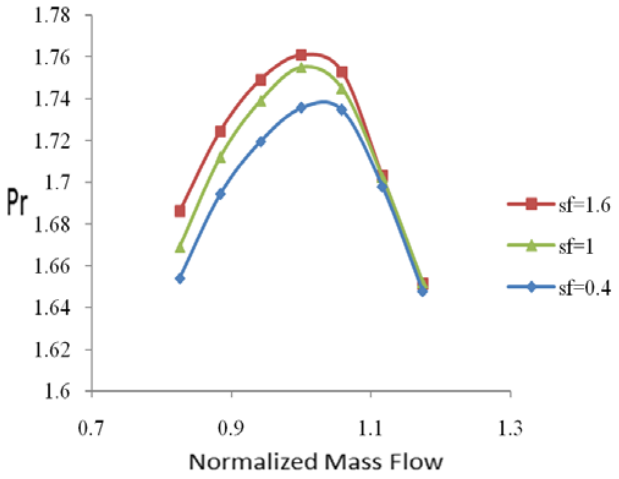

Fig. 11 Pressure ratio variations with mass flow for three SF cases

Comparison of entropy distributions on rotor suction side and stator pressure side, with reference value from airflow inlet area, are shown in Figs. 12 and 13, respectively. As can be seen, regions of large entropy changes are located near rotor trailing edge and stator leading edge, which indicates more energy loss happens in that area for all three cases. However, a comparatively bigger area of large entropy is observed for SF=0.4 case, which indicates more energy loss is occurring and this explains lower efficiency is obtained for miniaturized model. Results from designed mass flow are used for this comparison analysis.

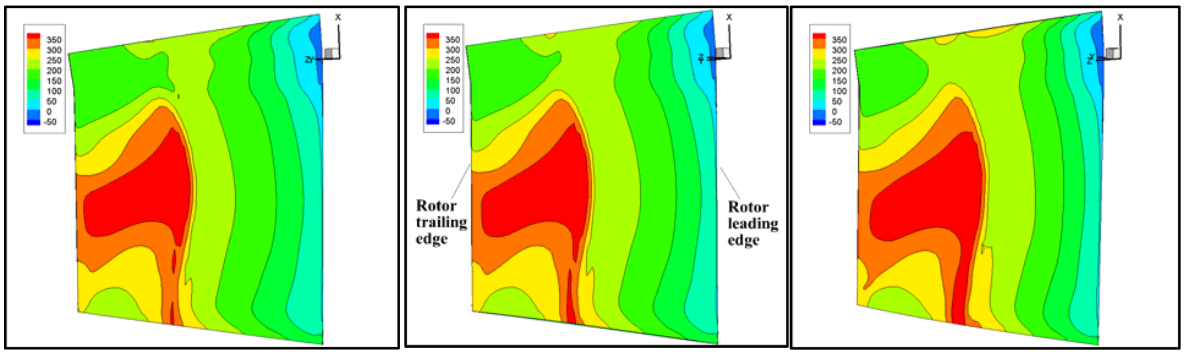

SF=1.6 SF=1 SF=0.4

Fig. 12 Comparison of entropy distributions on R_{ss} during its miniaturization process

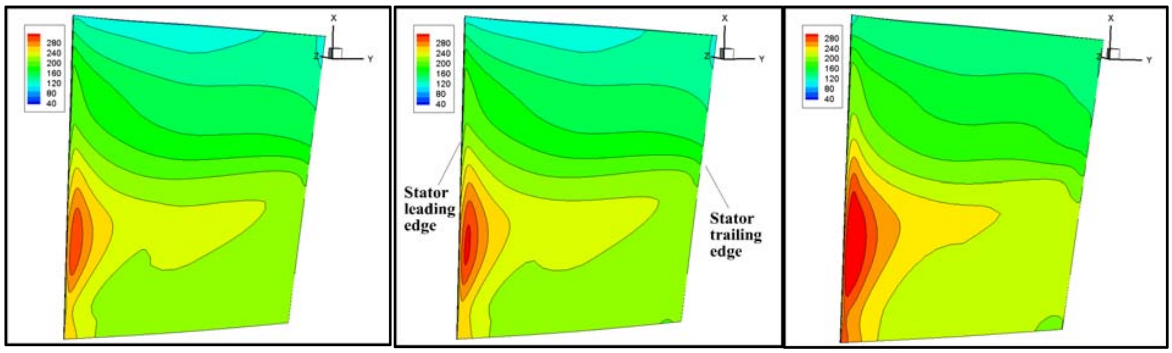

SF=1.6 SF=1 SF=0.4

Fig. 13 Comparison of entropy distributions on S_{ps} during its miniaturization process

IV. Wall Heat Flux Effect

As a miniature gas turbine is expected to have more heat losses due to the higher surface-to-volume ratio, we will now study the influence of the wall heat transfer on the compressor performance. The adiabatic wall condition, which used for previous study, is replaced with a specified heat transfer coefficient on all wall boundaries. The heat exchange is thus allowed to occur between fluids within compressor domain and air in its surrounding environment. The same thermal boundary conditions are applied on all wall boundaries for SF=1.6, SF=1 and SF=0.4 cases at their designed mass flow. Specifications of the thermal condition and comparison of numerical results are given in Table III below:

TABLE III
Comparisons of Different Thermal Conditions

Heat transfer coefficient(w/m^2×k)			200	
Free stream Temperature(k)			288	
SF	Pr	Change of Pr	η_{ad}	Change of η_{ad}
1.6	1.760264	-0.03%	0.783879	+0.68%
1	1.751108	+0.02%	0.777988	+1.00%
0.4	1.734521	-0.06%	0.765332	+1.02%

As listed in Table III, for non-adiabatic wall conditions, the pressure change is insignificant for three cases studied, thus the effect of heat transfer on it is negligible. However, there is a slight increase of efficiency, with the largest increase observed for SF=0.4 case. For miniature compressor, the increase of surface-to-volume ratio also contributes to an increased heat transfer through wall. The compressor internal temperature will decrease consequently, which leads to smaller entropy change, with reference to the value at airflow inlet surface. Figs. 14, 15 respectively present distributions of temperature and entropy on rotor blade when adiabatic and non-adiabatic wall conditions are applied. Although high temperature and large entropy regions locate at almost the same area for both wall conditions, the decrease of the extend of high value area for these two properties are obvious. This explains the increase of efficiency when non-adiabatic wall conditions are applied. The results from benchmark case are used for this comparison.

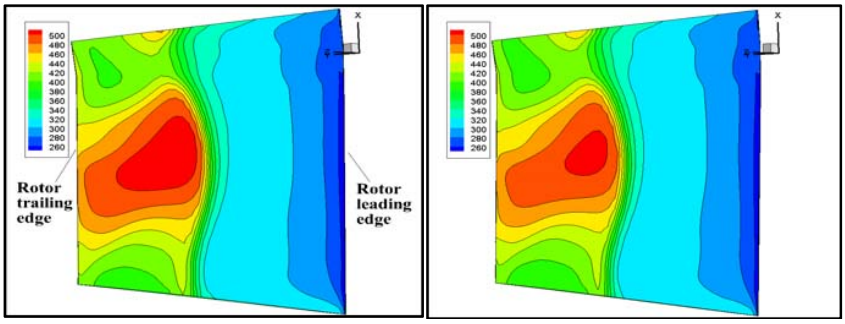

Adiabatic wall condition Non-adiabatic wall condition

Fig. 14 Comparison of temperature distributions on R_{ss} with different wall thermal conditions

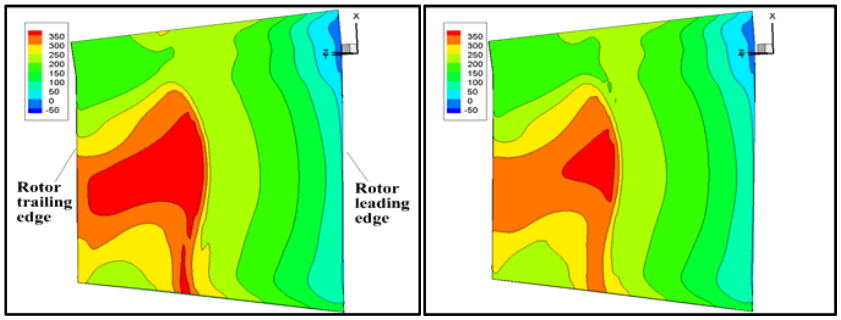

Adiabatic wall condition Non-adiabatic wall condition

Fig. 15 Comparison of entropy distributions on R_{ss} with different wall thermal conditions

V. Conclusions

The miniaturization of gas turbines leads to smaller operating Reynolds number and higher heat losses. In the present work, the influence of these effects on the performance of an axial compressor is computationally studied. The scaling effect on compressor efficiency and performance is our main concern.

Our results show, that the Reynolds number is the key impact factor on compressor performance and efficiency. A decrease of pressure ratio and efficiency is observed when Reynolds number decreases, i.e., when compressor is miniaturized. This is due to the increased entropy change when model size goes down and the increasing importance of the viscosity, which leads to higher viscous losses. This is in consistence with the experience that drops of performance and substantial loss of efficiency is observed for gas turbine engine at small scale. The optimization of compressor blade geometry is suggested to avoid high entropy regions when a miniaturization is required.

The heat transfer is another issue which cannot be ignored for compressor miniaturization practice. Compressor performance, however, is not significantly affected by the wall heat transfer. More energy loss through wall is observed for compressor at small scale, which leads to more cooling of compressor blade, which may actually benefit its overall efficiency within our studied scope. Thus compressor cooling is suggested, if feasible, to enhance compressor efficiency.

With these results, the computational methods described here can be used for the optimization of miniature gas turbines.

Acknowledgment

Special thanks to the Defense Science Organization for its financial support of this study.

References

[1] Wang, Y.-F. and J. Hu, *Effects of Reynolds number on performance and stability of axial fans/compressors.* Nanjing Hangkong Hangtian Daxue Xuebao/Journal of Nanjing University of Aeronautics and Astronautics, 2004. 36(2): p. 145-149.

[2] Choi, M., et al., *Effects of the low Reynolds number on the loss characteristics in an axial compressor.* Proceedings of the Institution of Mechanical Engineers, Part A: Journal of Power and Energy, 2008. 222(2): p. 209-218.

[3] Back, S.C., et al. *Effect of surface roughness location and reynolds number on compressor cascade performance*. in *ASME Turbo Expo 2010: Power for Land, Sea, and Air, GT 2010, June 14, 2010 - June 18, 2010*. 2010. Glasgow, United kingdom: American Society of Mechanical Engineers.

[4] Casey, M.V. and C.J. Robinson. *A unified correction method for Reynolds number, size, and roughness effects on the performance of compressors*. 2011. 55 City Road, London, EC1Y 1SP, United Kingdom: SAGE Publications Ltd.

[5] Zheng, X., et al., *Effects of Reynolds number on the performance of a high pressure-ratio turbocharger compressor.* Science China. Technological Sciences, 2013. 56(6): p. 1361-9.

[6] Chen, L., F. Sun, and C. Wu, *Effect of heat resistance on the performance of closed gas turbine regenerative cycles.* International Journal of Power and Energy Systems, 1999. 19(2): p. 141-145.

[7] Tyagi, S.K., et al., *Effect of several irreversibilities on the thermo-economic performance of a realistic Brayton heat engine cycle.* Indian Journal of Pure and Applied Physics, 2005. 43(8): p. 612-19.

[8] Rongliang, Z., et al., *The steady-state modeling and optimization of a refrigeration system for high heat flux removal.* Applied Thermal Engineering, 2010. 30(16): p. 2347-56.

[9] Ma, Y. and G. Xi. *Effects of reynolds number and heat transfer on scaling of a centrifugal compressor impeller*. in *ASME Turbo Expo 2010: Power for Land, Sea, and Air, GT 2010, June 14, 2010 - June 18, 2010*. 2010. Glasgow, United Kingdom: American Society of Mechanical Engineers.

[10] Schluter, J.U., et al., *A framework for coupling reynolds-averaged with large-eddy simulations for gas turbine applications.* Journal of Fluids Engineering, 2005. 127: p. 806-815.

[11] Reid, L. and R.D. Moore, *Performance of single-stage axial-flow transonic compressor with rotor and stator aspect ratio of 1.19 and 1.26, respectively, and with design pressure ratio of 1.82.* NASA Technical Paper, 1978. 1338.

[12] Reid, L. and R.D. Moore, *Design and performance of four highly loaded, high speed inlet stages for an advanced high pressure ratio core compressor.* NASA Technical Paper, 1978. 1337.

[13] Chen, J., M.D. Hathaway, and P. Herrick, *Pre-stall behavior of a transonic axial compressor stage via time-accurate numerical simulation.* 2008.

[14] Burge, J.C., *Gas turbine compressors MID&AFT stage radial clearance control.* AIAA, 2004. 3416.

[15] Zante, D.E.V., A.J. Strazisar, and J.R. Wood, *Recommendations for achieving accurate numerical simulation of tip clearance flows in transonic compressor rotors.* NASA/TM, 2000(210347).

[16] Wiesner, F.J., *New Appraisal of Reynolds Number Effects on Centrifugal Compressor Performance.* American Society of Mechanical Engineers (Paper), 1978(78 -GT-149).